Informatics and Control Problems 45 Issue 2 (2025)
journal homepage: www.icp.az

Development of the FPR-5 intelligent dynamometer chart transmitter

Yaver Aliyev

Institute of Control Systems, Baku, Azerbaijan

ARTICLE INFO

Article history:
Received 01.09.2025
Received in revised form 17.09.2025
Accepted 29.09.2025
Available online 26.12.2025

Keywords:
Piezoresistive
Piezoelectric
Strain gauge
Accelerometer
Dynamometer chart
Messdose
Calibration
Compression calibration bench
Load-signal graph
Stroke-signal graph
Systematic and random errors

ABSTRACT

The selection of the correct operating mode of sucker rod pumping units has a significant impact on the efficiency of oil production. In current practice, the inductive transducers used in traditional dynamometric measurements are technologically outdated; their element base is limited, their accuracy and speed are low, and the measurement method does not meet modern requirements. This complicates real-time control and diagnostics. Therefore, it is proposed to develop an intelligent dynamometer chart transmitter installed between the traverses to ensure accurate control and diagnostics in real-time. The proposed dynamometer chart transmitter records the force acting on the rod string with a piezoresistive strain gauge, and the displacement with a piezoelectric accelerometer. By combining a microprocessor, communication module, measurement electronics and accumulator into a single housing, a modern measurement system is obtained that possesses high accuracy, reliability and ease of application in industrial conditions.

1. Introduction

One of the most effective methods for monitoring the operating modes of sucker rod pumping units (SRPUs) and studying the operating mode of the pump is the study of well dynamometer charts. This method allows determining the state of fullness of the pump cylinder, the pump cylinder fill level, the tightness of the suction and discharge valves, the influence of gas, plunger seating, pipe integrity, rod breakage or opening, plunger jamming, polished rod stroke, rod load, and other process parameters [1, 2, 3].

The primary equipment in deep-well automation systems are dynamometer sensors and their data recording devices. These tools provide the necessary information for analyzing the operating modes and malfunctions of sucker rod pumping units.

Thus, the accuracy of the dynamometer chart transducers used in SRPU-operated wells and their correct presentation of the actual state of the pump are one of the conditions ensuring the reliability of diagnostic systems.

2. Problem statement

Dynamometer chart data is mainly obtained through stroke and force transducers.

The stroke transducer determines the movement parameters of the rod string - the stroke length

*Corresponding author.
E-mail addresses: aliyevyaver@gmail.com (Y.G. Aliyev)

www.icp.az/2025/2-08.pdf https://doi.org/10.54381/icp.2025.2.08
2664-2085/

of the suspension point, the oscillation period, and the moments when the string passes through the lower and upper dead centers.

The force transducer measures the total load acting on the polished rod. This load is the sum of the weight of the fluid and rods being lifted from the well, as well as the friction forces generated in the pump and tubing.

The creation of dynamometer chart transducers requires a complex and comprehensive approach. In this process, the latest achievements in such fields as strain gauging, microelectronics, mathematical signal processing, metrology and reliability should be used. The analysis of dynamometer charts shows that the most important issue in studying the operating modes and malfunctions of the SRPU is the creation of force transducers. Because these transducers have strict requirements for sensitivity, accuracy, reliability, structural simplicity and ease of installation.

Dynamometer chart transducers differ from each other in terms of their mounting locations on the SRPU, their structural design, and measurement methods [4].

- In dynamometers mounted on the balance beam (force) or on the roller bearing of the balance beam (stroke), an induced electromotive force (EMF) is generated proportional to the displacement of the inductor core.
- In analog inductive transducers, the EMF generated by the displacement of the inductor core is transmitted to the well control unit (WCU) as a voltage varying in the range of 0…15V, rectified and measured by bringing it to a constant reference voltage V_{Ref} (Reference Voltage) – the reference voltage determines the maximum voltage limit that the analog to digital converter (ADC) can measure and is a constant reference level for evaluating the measured analog signal [5].
- In frequency inductive transducers, the oscillations generated by the displacement of the inductor core are converted into continuous frequency signals in the range of 1700…3200Hz and transmitted to the WCU.

Since the load is determined indirectly, rather than directly, by the bending strain of the balance beam, the measurement accuracy is limited. As a result of this limitation, the dynamometer chart curves do not fully reflect the actual technological state of the pumping unit.

Although the hydraulic transducers of the messdose type directly determine the load acting on the rod, they have a complex structure. Their composition, such as a housing, membrane, piston, oil chamber, capillary tube, etc., complicates operation. In such transducers, constant monitoring of tightness, regular calibration and testing are necessary. Otherwise, the measurements are distorted.

These characteristics are considered to be the shortcomings of inductive and messdose type transducers. This, in turn, makes the development of intelligent dynamometer chart transducers based on the piezoresistive effect relevant from a scientific and practical point of view, since this type of transducers significantly improves the temperature stability, linearity, and calibration capabilities of measurements.

3. Solution

The article addresses the development of a new intelligent dynamometer chart transmitter (IDT) based on a piezoresistive force sensor (measurement range 5t) and a piezoelectric stroke sensor (measurement range 10g) to overcome the shortcomings of inductive and messdose type transducers. The device includes an SM103-OPA-DIF controller module, an SC2-5 force sensor, a Kistler-K8315A stroke accelerometer, a LoRa F8L10C RF (radio frequency) transceiver, and a rechargeable battery. The accelerometer's internal temperature sensor is used to make adjustments for load and temperature changes. The block diagram of the FPR-5 IDT that meets these requirements is presented in **Fig. 1.**

The intelligence of the IDT is provided by the following functions implemented in its

microcontroller based control and signal processing module:

- Automatic compensation of the influence of the temperature factor on the measurement results;
- Execution of calibration and self-diagnostic procedures at the software level;
- Digital processing, filtering and correction of analog signals;
- Transmission of measurement results and service data via digital interface.

Due to these functions, the FPR-5 (Force–Position Radio transmitter) intelligent dynamometer chart transmitter is used not only as a sensor that measures physical quantities, but also as an intelligent information-measuring device that ensures the reliability and accuracy of information.

Thus, the FPR-5 IDT, created on the basis of the integration of all functional nodes in a single housing, is designed to accurately measure the force acting on the polished rod and the rod's stroke path, process it according to the algorithm, and transmit it.

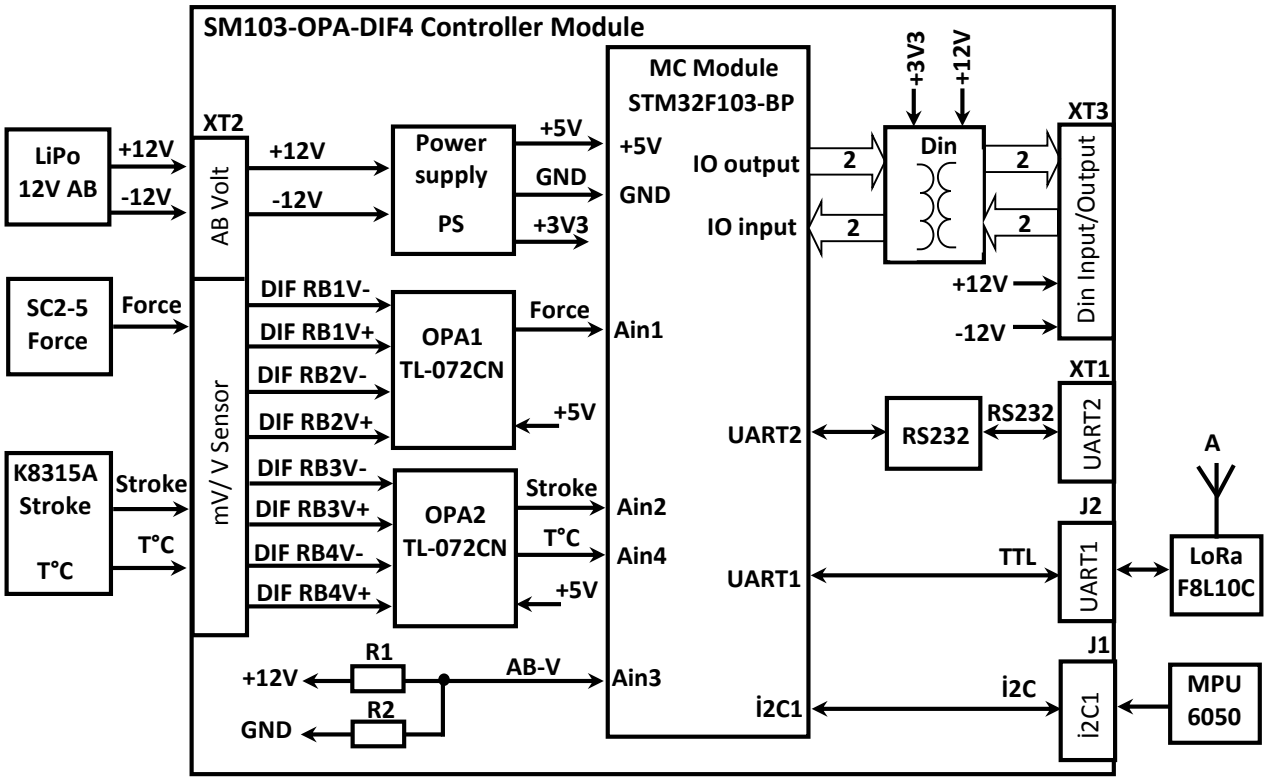

Fig. 1. Block diagram of the FPR-5 IDT

FPR-5 IDT consists of the following main functional nodes:

- SM103-OPA-DIF4 controller module;
- LoRa F8L10C transceiver module;
- LiPo rechargeable battery;
- SC2-5 piezoresistive force sensor;
- K8315A Kistler piezoelectric stroke sensor;
- MPU-6050 inertial measurement sensor.

SM103-OPA-DIF4 multifunction controller module (later SM103) integrates all functional nodes of the FPR-5 IDT with an STM32-based MC, combines electricity on a single printed circuit board, adjusts signal levels, and connects with peripheral devices (radio, sensors, etc.). The SM103 controller receives and pre-processes signals from force and stroke transducers, digitizes of analog

signals, and forms the necessary data in memory for constructing a dynamometer chart.

The data processed in the controller is transmitted via RF channel to the WCU or to a higher level - the MDM computer - for plotting a dynamometer chart graph.

The reliable and efficient operation of the FPR-5 IDT largely depends on the correct choice of the microcontroller. For this purpose, the 32-bit ARM-Cortex-M3 core STM32F103C8T6-BP STAMP type module (later STM32-STAMP) was selected as an efficient and multifunctional microcontroller platform for the SM103 [6].

The STM32-STAMP is a compact (22.5 x 53 mm) plug-in MC that connects to the SM103 module via a 40-pin connector and integrates into the main system.

The STM32 family, which has a multilayer and multiprocessor structure, has an NPU (numeric processing unit) and FPU (floating point unit) are distinguished by their processing of integer and fractional numbers, parallel operation of various functions, embedded encoder, and high integration capabilities [7].

The LoRa radio transceiver module is used to establish communication and exchange data between the FPR-5 IDT and other control controller modules or a computer.

For this purpose, the Lora F8L10C radio transceiver module with dimensions of 24.4x37.5x4.2mm and operating frequency range of 410…441MHz was selected [8, 9]. The radio transceiver is connected to the J2 connector of the SM103.

The rechargeable battery provides the nodes of the FPR-5 IDT with the necessary stabilized voltages. Due to the low power requirement of FPR-5 IDT, it can be powered by a +12V 3400mAh Lithium Polymer (LiPo) battery for a long time. The +12V output of the LiPo battery is converted to +5V and +3.3V constant voltage with appropriate stabilizers and powers all nodes.

The SC2-5 piezoresistive load cell provides force information by converting the resistance change of its internal bridge element into a corresponding voltage (mV) signal proportional to the deformation caused by the mechanical compression force of the load applied to the suspension point of the SRPU and transmitting it to the analog input A_{in1} of the MC [10-12].

A general view of the SC2-5 sensor is shown in **Fig. 2**, the load-signal graph is shown in **Fig. 3**, and the technical parameters and cable connections are given in **Table 1**.

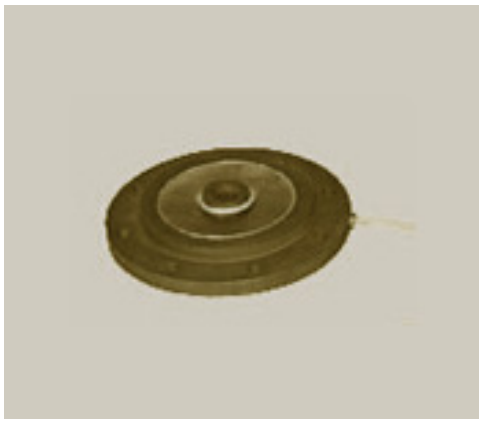

Fig. 2. SC2-5 load cell

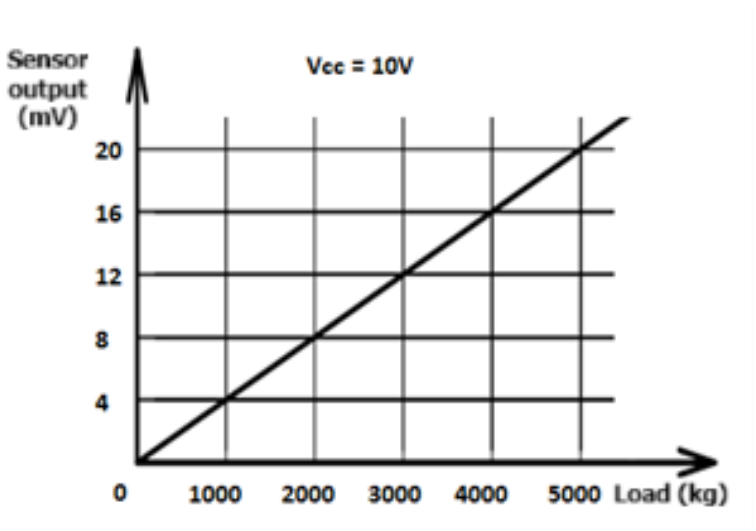

Fig. 3. Load-signal graph of SC2-5

Table 1

Technical parameters and cable connections of SC2-5 load cell

SC2-5 technical parameters			**SC2-5 cable connections**		
Maximum load, tons	5		Signal+	Twisted pair	Terminal
Accuracy class	C1		Signal-		
Rated sensitivity at max load, mV/V	2		Power supply +	Paired wires	Terminal
Operating temperature range,℃	-30...+50		Power supply-		
Maximum load limit,%	150		Shield	No connection to the housing	
Breaking load limit,%	400				
Constant power supply voltage, max, V	12				
Input resistance, Ohm	750				
Output resistance, Ohm	700				
Protection rating	IP67				

As can be seen from the load-signal graph in Fig. 3, when a maximum load of 5 tons is applied, the load-signal dependence of the SC2-5 sensor with a transfer coefficient of 2mV/V and a power supply voltage of +10V is linear. This confirms its high measurement accuracy and, as a result, allows the sensor to be widely used in various measuring devices.

Continuous control of the supply voltage is an important condition for maintaining the measurement accuracy of the SC2-5 sensor. The proposed FPR-5 IDT is powered by an alternative power source – AB (V_{AB}) as a completely independent measuring device. The nominal voltage of AB is V_{AB} =12V when fully charged, but it begins to decrease as energy is consumed during use.

V_{out} of the SC2-5 load cell varies depending on the power supply voltage: for example, the output signal of the sensor with an applied load of 5 tons, a rated sensitivity k=2mV/V and a battery voltage of V_{AB} =12V is V_{out} =12V×2mV/V=24mV. But if the current value of the AB voltage under the same load drops to V_{AB}=8V, it will be V_{out} =8V×2mV/V=16mV. If there is no correction for the measurement due to the change in V_{AB}, the same load will be incorrectly expressed with different values at different voltages. Temperature changes also affect the accuracy of the measurement parameters.

For this reason, the controller monitors the AB voltage and temperature values for the accuracy of the measurement results, and adjustments are made to the dynamometer chart parameters based on the changes.

Structurally, the SC2-5 load cell is installed between two specially designed horseshoe-shaped plates for easy access to the well rod. The sensor body is fixed to the lower plate with 8 screws, and the sensitive measuring element is fixed to the upper plate with 1 screw. In order to fully transfer the force generated during compression to the measuring mechanism, slots are opened at the ends of the plates for placing steel rods that perform the link function.

Kistler-8315A-010-BT-TB Piezoelectric effect acceleration sensor is designed to provide stroke information by converting the electric load change of its internal capacitance element into an appropriate voltage (mV) proportional to the +/−10g acceleration generated during the up-down dynamic movement of the suspension point of the SRPU and transmitting it to the A_{in2} analog input of the MC [13, 14].

The temperature sensor embedded in the K8315A provides temperature information by converting the internal temperature of the IDT body into voltage (mV) and transmitting it to the A_{in4} input of the MC.

The general view and dimensions of the K8315A accelerometer are given in **Fig. 4**.

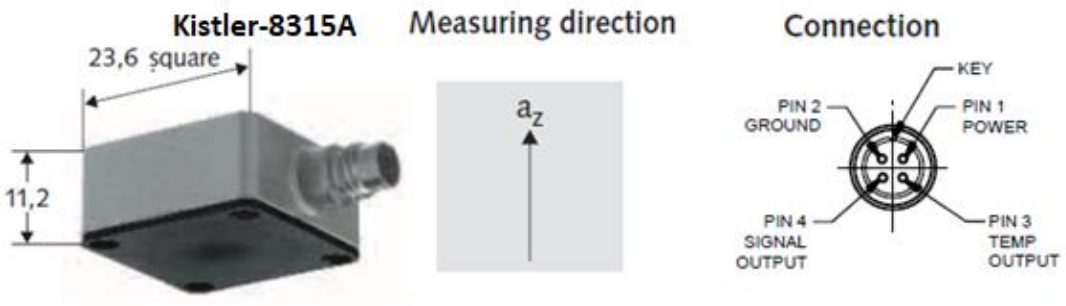

Fig. 4. View of the K8315A accelerometer

Brief technical specifications of the K8315A accelerometer sensor:

- Supply voltage: +5…+50VDC constant voltage;
- Output signal: +1.65V +/-1.65V analog unipolar;
- Measuring range: 0...+/−10g;
- Output signal corresponding to “0g”: +1.65V;
- Sensitivity: 200 mV/g;
- Resolution: 380 µg/LSB;
- Operating temperature: −40°C…+85°C;
- Dimensions: 18.8 x 23.6 x 11.2 mm.

MPU-6050 MEMS accelerometer module is a micro-electro-mechanical system (MEMS) comprised of 3-axis acceleration, 3-axis compass and temperature sensors. MPU-6050 is a small, 14x21mm, module with serial I2C interface that allows measuring the acceleration, velocity, orientation, displacement and temperature of any object [15, 16].

As an alternative to the K8315A analog measuring sensor, the MPU-6050 with digital interface can be used to determine the stroke path by recording the moments when the rod passes through the bottom and top dead points based on the value of the movement acceleration. The MPU-6050 sensor can also measure temperature.

The general view of the proposed monolithic body of the FPR-5 IDT is shown in **Fig. 5**, and its structural layout is shown in **Fig. 6**:

Fig. 5. General view of the FPR-5 IDT

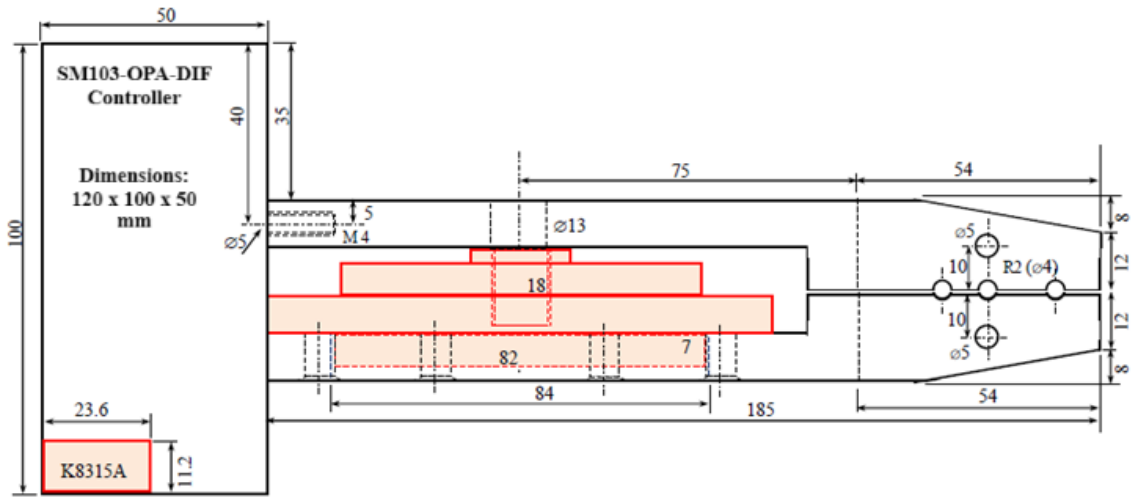

Fig. 6. Structural layout of FPR-5 IDT

Dynamometer transducers used in SRPU-operated wells must withstand continuous exposure to moisture, sulfur, and other corrosive factors over a wide temperature range for long periods of time, be resistant to overload, and operate in hazardous areas [17].

Therefore, it is proposed to create an IDT in a monolithic body with a fire and explosion protection design for operation in harsh environments. The design of the device meets the degree of air-tight protection, which ensures its reliable operation in open oilfield areas.

The sensors used in the FPR-5 IDT provide the well data necessary for constructing dynamometer chart curves that allow studying the operating conditions and operating mode of the SRPU, and the features of measuring their analog outputs through the ADC are described below.

The analog signal measurement process is performed by the internal ADC module of the STM32-STAMP controller module. The converted output voltages of the force, stroke, AB and T°C sensors are entering to the Ain1, Ain2, Ain3 and Ain4 inputs, respectively.

The maximum measurement limit of the ADC is V_{Ref} = 3.3V, and the conversion degree is 12-bit.

In order to accurately read signals from piezoresistive bridge sensors, the measurement limit of the measuring device must be matched to the measured quantity. For this purpose, a matching scheme using an operational amplifier (OA) and a voltage divider (VD) has been selected **(Fig. 7)**. As a result, the signal enters the ADC in the appropriate range and digitization accuracy is ensured.

According to Fig. 7, the function of the OA is to amplify the "millivolt" level bipolar or unipolar output signals received from the piezoresistive bridge circuit many times over.

In the piezoresistive element, RB_1 ...RB_4 are the bridge arm resistances, V+ is the power supply voltage input, and the difference V_1 - V_2 is the voltage output amplified by the OA.

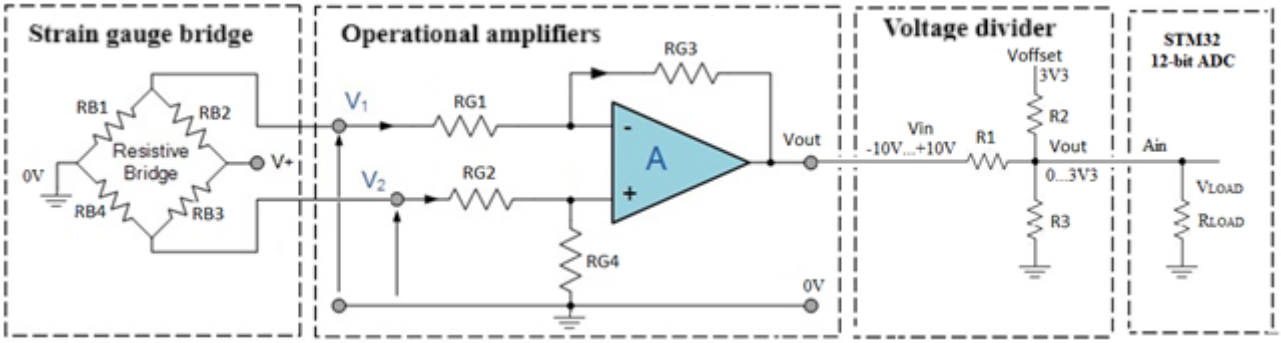

Fig. 7. Piezoresistive sensor output interface diagram with ADC block

In the presented two-input amplification scheme, one side of the voltage signal (V_1) is fed to one input of the amplifier, and the other side (V_2) to the second input, and the resulting output voltage V_{out} will be amplified proportional to the difference between the input voltages V_1 and V_2 (V_1 - V_2) [18].

In the OA circuit, the value of the gain coefficient G ("gain") is determined by selecting the resistances RG_1 ...RG_4, taking into account the condition RG_1=RG_2 and RG_3=RG_4. In this case, the ranges of voltage changes occurring at the outputs of the piezoresistive bridge, OA and VD circuit parts must be taken into account.

The piezoresistive bridge circuit forms the initial signal output in a small voltage range (0…20mV) corresponding to the applied load. This signal, when passing through the OA, changes in the bipolar voltage range (–10V…+10V). Thus, the total variation range of the OA output voltage is 20V=20000mV. The amplification factor of the OA is calculated as follows:

$$G = \frac{20000mV}{20mV} = 1000$$

The gain of 1000 is achieved by selecting the resistances RG_1=RG_2=1kΩ and RG_3=RG_4=1000kΩ in the OA (RG_3/RG_1=1000).

Then, the bipolar signal from the output of the OA enters the VD, which consists of three resistors to which a reference voltage of 3.3V_{Ref} is applied. The equivalent circuit of the VD is depicted in **Fig. 8.**

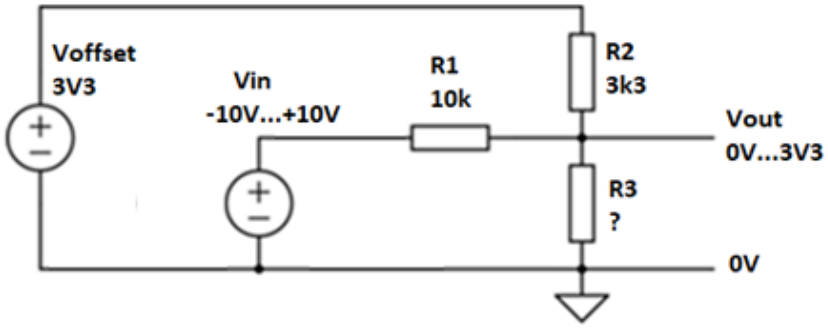

Fig. 8. Equivalent circuit of a voltage divider

Function of VD is to bring the bipolar output signal in the range of the ADC (–10V ... +10V) to the unipolar input measurement voltage range of the ADC (0V...3.3V) [19].

When applying the principle of superposition - the addition of signals (voltages or currents) - the values of the resistances R_{eq} and R_3 are determined from the three-resistor voltage divider formula as follows:

$$Vout = \left(\frac{V1}{R1} + \frac{V2}{R2}\right) \times (R1 \parallel R2 \parallel R3)$$

According to the VD scheme, the equivalent (R_{eq}) value of the parallel-connected resistances R_1, R_2, and R_3 is determined as follows:

$$Req = R1 \parallel R2 \parallel R3 = \frac{1}{\frac{1}{R1}+\frac{1}{R2}+\frac{1}{R3}} = \frac{R1R2R3}{R1R2+R1R3+R2R3} \quad (1)$$

Since there are two unknowns (R_3 and R_{eq}) in formula (1), let us first use Kirchhoff's law to determine the resistance R_{eq}.

According to Kirchhoff's law, the algebraic sum of the currents at each electrical node is zero, so that, the sum of the currents entering a junction is equal to the sum of the currents leaving it:

$$\frac{V_1}{R_1}+\frac{V_2}{R_2}=\frac{V_{out}}{R_{eq}}$$

$$\frac{V_1\times R_2+V_2\times R_1}{R_1\times R_2}=\frac{V_{out}}{R_{eq}}$$

$$V_{out}\times R_1\times R_2=R_{eq}\times(V_1\times R_2+V_2\times R_1) \quad (2)$$

$$R_{eq}=\frac{V_{out}\times R_1\times R_2}{V_1\times R_2+V_2\times R_1}$$

$$R_{eq}=\frac{3.3V\times 10k\times 3.3k}{10V\times 3.3k+3.3V\times 10k}=\frac{108.9}{66}=1.65\ k\Omega$$

From knowing R_{eq} =1.65kΩ as a result of applying Kirchhoff's law, the resistance R_3 can be calculated according to formula (1):

$$R_3=\frac{R_{eq}\times R_1\times R_2}{R_1\times R_2-R_{eq}\times R_1-R_{ekv}\times R_2}$$

$$R_3=\frac{1.65k\times 10k\times 3.3k}{10k\times 3.3k-1.65k\times 10k-1.65k\times 3.3k}=\frac{54.45}{11.055}=4.925\ k\Omega$$

Thus, in order to obtain the output voltage of the VD in accordance with the requirements specified in the report, it is advisable to select a resistance of R_3 =4.925kΩ in the circuit.

As a result of the correct selection of R3, the equivalent resistance is R_{eq} =1.65kΩ. As a result, the unipolar voltage brought to the measurement range (0…3.3V) is transmitted from the output of the VD to the last stage and enters the 12-bit ADC input of the STM32 MC. Thus, for accurate measurement of the analog signal, it is ensured that the signal is brought to the correct range when transmitted from the VD output to the ADC input of the STM32 MC.

From R_{eq}=1.65kΩ as a result of the application of Kirchhoff's law, the output voltage V_{out} of the VD is determined using formula (2):

$$V_{out}=\frac{R_{eq}\times(V_1\times R_2+V_2\times R_1)}{R_1\times R_2} \quad (3)$$

Based on formula (3), let us calculate the output voltage V_{out} of the VD at different values of the input voltage V_1 of the VD ($V_{in.min}$, $V_{in.0}$ and $V_{in.max}$):

1. If $V_1 = V_{in.min}$ = –10V:

$$V_{out.min}=\frac{R_{eq}\times(V_1\times R_2+V_2\times R_1)}{R_1\times R_2}=\frac{1.65k\times(-10V\times 3.3k+3.3V\times 10k)}{10k\times 3.3k}=0V$$

2. If $V_1 = V_{in.0}$ = 0V:

$$V_{out.0}=\frac{R_{eq}\times(V_1\times R_2+V_2\times R_1)}{R_1\times R_2}=\frac{1.65k\times(0V\times 3.3k+3.3V\times 10k)}{10k\times 3.3k}=1.65V$$

3. If $V_1 = V_{in.max} = +10V$:

$$V_{out.max} = \frac{R_{eq} \times (V_1 \times R_2 + V_2 \times R_1)}{R_1 \times R_2} = \frac{1.65k \times (10V \times 3.3k + 3.3V \times 10k)}{10k \times 3.3k} = 3.3V$$

The results show that when the input voltage of the VD changes in the range of –10V…+10V, the signal transmitted from its output to the ADC is formed in the range of 0…3.3V. In this case, the voltage level of +1.65V corresponds to the "0V" value of the VD input signal and is considered as the "zero line" and determines the boundary of the change in the polarity of the signal.

The amplification factor G of VD is determined by the following formula:

$$G = \frac{V_{out.max} - V_{out.min}}{V_{in.max} - V_{in.min}} = \frac{3.3V - 0V}{10V - (-10V)} = \frac{3.3}{20} = 0.165$$

According to the scheme of coordination with the ADC block, the measured voltage V_{load} is expressed by the following formula:

$$V_{load} = \frac{R_{load}}{R_{load} + R_{eq}} \times V_{outVD}$$

In order to obtain error-free measurement results, the input (V_{load}) voltage of the ADC and the output (V_{outVD}) voltage of the VD must have approximately the same value ($V_{load} = V_{outVD}$).

The main condition for meeting this requirement is expressed as follows:

$$R_{load} \gg R_{eq} \quad or \quad R_{inADC} \gg R_{outVD}$$

that is, the input load resistance of the ADC must be significantly greater than the output resistance of the source.

According to the technical characteristics of the STM32 MC, the input load resistance of the ADC is R_{load} =50kΩ. This value is much larger than the output resistance of the VD R_{eq} =1.65kΩ, and small changes in the measured voltage V_{load} due to parallel effects can be ignored. However, if high accuracy is required, a small V_{offset} correction should be applied to the final V_{load} result.

Numerous application notes for ADCs with high input resistance recommend that their inputs be powered from sources with relatively low resistance [20].

In the STM32-STAMP controller module, the converted output voltages of the force, stroke, AB and T°C sensors are read and processed from the A_{in1}, A_{in2}, A_{in3} and A_{in4} inputs of the ADC, respectively, in the following order:

- The maximum conversion code (N_{max}) of a 12-bit ADC is calculated as:

$$N_{max} = 2^{12} = 4096$$

- For V_{Ref} =3.3V, the voltage equivalent of 1-bit code (mV_of_1bit) is determined:

$$mV\_of\_1bit = \frac{V_{Ref}}{N_{max}} = \frac{3300mV}{4096} = 0.805664mV/bit$$

- The converted code of the AB power supply voltage (N_{AB}) is read from the A_{in3} input and the current value of the voltage V_{AB} (V) is determined:

$$V_{AB} = mV\_of\_1bit \times N_{AB}$$

- Based on the voltage V_{AB} and the rated sensitivity of the force sensor k=2mV/V, the maximum current output signal of the transducer corresponding to the nominal load, $_{max}$ (mV), is calculated:

$$V_{max} = V_{AB} \times k$$

- For Q_{max} =5t, the load kilogram equivalent of 1mV voltage (kg_of_1mV) is determined:

$$kq\_of\_1mV = \frac{Q_{max}}{V_{max}}$$

- The converted code of the output voltage of the SC2-5 sensor corresponding to the current load (N_{load}) is read from the input $A_{in1.}$ According to the N_{load} code and the voltage equivalent of the 1-bit code (mV_of_1bit), the output voltage of the sensor corresponding to the current load V_{load} (mV) is determined:

$$V_{load} = mV\_of\_1bit \times N_{load}$$

- The weight of the applied current load Q_{load} (kg) is determined by the V_{load} voltage and the load equivalent of 1mV voltage (kg_of_1mV)

$$Q_{load} = kg\_of\_1mV \times V_{load}$$

- The converted code (N_g) of the output voltage of the K8315A sensor corresponding to the current acceleration is read from the input A_{in2}. According to the N_g code and the voltage equivalent of the 1-bit code (mV_of_1bit), the output voltage of the sensor corresponding to the current acceleration is determined as V_g (mV):

$$V_g = mV\_of\_1bit \times N_g$$

- Since the output voltage $V_{g.max}$=1.65V corresponding to the acceleration G_{max}=10g in the K8315A sensor, the voltage equivalent of the 1g acceleration (mV_of_1g) is determined:

$$mV\_of\_1g = \frac{1650mV}{10g} = 165mV/g$$

- Given the voltage V_g and the voltage equivalent of 1g acceleration (mV_of_1g), the current acceleration G_{cur} (g) is determined:

$$G_{cur} = \frac{V_g}{mV\_of\_1g} = \frac{V_g mV}{165mV/g}$$

- The converted code (N_t) of the T°C output voltage of the K8315A sensor corresponding to the internal temperature of the transmitter body is read from the A_{in4} input. Based on the N_t code and the voltage equivalent of the 1-bit code (mV_of_1bit), the current T°C output voltage V_t (mV) of the transmitter is determined:

$$V_t = mV\_of\_1bit \times N_t$$

- Based on the voltage V_t, the current temperature value T°C is calculated in the K8315A sensor using the following formula:

$$T°C = \frac{V_t - 0.424}{0.00625}$$

Thus, the conversion of analog signals into digital codes by the ADC and the reading of these codes constitute only the initial stage of the measurement process. First, based on the voltage equivalent of a single code, the corresponding voltage values for each parameter are calculated, and then these voltages are converted into their physical equivalents for force (kg), acceleration (g), and

temperature (°C). Accurate determination of the conversion coefficients for each sensor is essential for the correct interpretation of measurements, calibration, filtering, and the formation of control decisions within the program algorithm. Consequently, the complete and correct execution of this sequence in the STM32-STAMP module is not only a fundamental requirement for ensuring measurement reliability and accuracy, but also a key factor in maintaining the stable operation of the control system.

4. Laboratory testing

To ensure quality and accuracy, inspection and calibration of measuring instruments should be carried out through testing laboratories.

Therefore, before use, the measuring tool FPR-5 IDT must be tested and calibrated by applying a load on a compression calibration bench (CCB) equipped with reference test and measurement equipment so that the dynamometer chart curves correctly reflect the condition of the submersible pump [21, 22].

The block diagram of the calibration of the FPR-5 IDT on a compression calibration bench with the equipment used for laboratory testing and the general view of the CCB are given in **Fig. 9**:

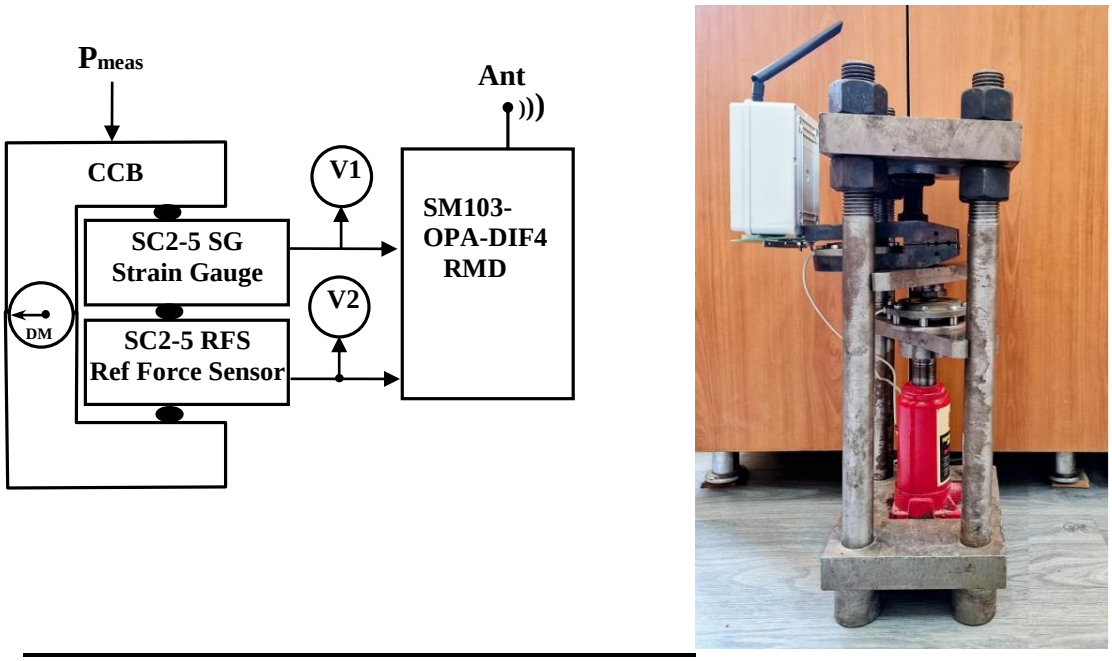

Fig. 9. Block diagram of IDT calibration and general view of CCB

Here: CCB – compression calibration bench; P_{meas} – value of compression force; DM – mechanical dynamometer indicator showing the value of P_{meas}; SC2-5 SG – 5-ton piezoresistive strain gauge; SC2-5 RFS – 5-ton piezoresistive reference force sensor; V_1 and V_2 – multimeters monitoring SG and RFS output voltages; SM103-OPA-DIF4 RMD – reference measuring device created on the basis of STM32F103; Ant – LoRa Radio Transceiver with antenna.

When the SG and RFS sensors are compressed in parallel between the plates of the CCB with the P_{meas} force, the converted voltage corresponding to the studied force, monitored by the multimeter V_1, is input to the analog inputs A_{in1} of the controller, and the converted voltage corresponding to the reference force, monitored by the controller V_2, is input to the analog inputs A_{in2}. The DM mechanical indicator on the CCB shows the value of the P_{meas} force corresponding to the applied load.

Methodology for processing experimental results. When processing the test results of force transducers, the first step is to determine the linear part of the signal, construct calibration curves, and perform a statistical analysis of the main systematic and random errors in the measurement. For this purpose, the least squares approximation is performed on the basis of experimental data, and statistical indicators such as RMS and dispersion are calculated [23-25].

The methodology for processing the experimental results of the FPR-5 IDT is also carried out in accordance with the above-mentioned procedure. After connecting the FPR-5 IDT to the power supply, it is necessary to wait at least 5 minutes so that a stable temperature setting is created as a result of the current flowing through the sensitive elements.

Before calibration, the SC2-5 load cell of the FPR-5 IDT must be loaded three times with maximum force (P_{max}). Each load must be applied for 1…2 minutes.

After the load has been completely removed, a minimum of 30 seconds must be waited and the force reset (P_0) must be recorded.

The measurement must be carried out in three stages at points corresponding to the predetermined values in the range (P_0...P_{max}): first in the loading range P_0...P_{max}, then in the unloading range P_{max}...P_0. There must be an interval of at least three minutes between each measurement stage and the measurements shall be taken at the same measurement points (i) during the loading-unloading process.

The measurement results are noted in **Table 2.**

Let us assume that the force P_{meas} was measured three times at point (i) and their values were different: U_L1, U_L2, U_L3 (loading) and U_U1, U_U2, U_U3 (unloading). The variation (V_i) at the considered measurement point (i) is determined by the modulus of the difference between the average values in the loading and unloading modes.

$$\mathrm{Vi} = \left|\frac{U_U1 + U_U2 + U_U3}{3} - \frac{U_L1 + U_L2 + U_L3}{3}\right|$$

The hysteresis error at the considered measurement point (i) is determined based on the maximum value of the variation as follows:

$$H = \pm\frac{max(Vi)}{2}$$

Table 2

Results of loading and unloading measurements of the SC2-5 sensor

Measure Point Number, i	Measure Load P_{meas}, tons	**Ref Force Sensor**	Measurements of the Reference and Load sensors at the Ain1 and Ain2 inputs of the controller were carried out under the following conditions: Supply voltage 12VDC; Load sensitivity 2.68mV/V and reference sensitivity 2.675mV/V; Max load limit of the press machine 8t.						**$U_{average}$**	**U_{force}** $U_{average}$ - $U_{average}0$ (1743.3)
		U_{Ref} mV	U_L1, mV	U_L2, mV	U_L3, mV	U_U1, mV	U_U2, mV	U_U3, mV	$U_{average}$, mV	U_{force}, mV
1	0	**0**	1743	1743	1744	1743	1743	1744	1743.3	0.3
2	1	**6.4**	1767	1767	1766	1767	1767	1766	1766.6	23.3
3	2	**12.8**	1787	1787	1788	1787	1787	1788	1787.3	44.0
4	3	**19.2**	1807	1807	1808	1807	1807	1808	1807.3	64.0
5	4	**25.6**	1828	1828	1829	1828	1828	1829	1828.3	85.0
6	5	**32**	1850	1849	1851	1850	1849	1851	1850.0	106.7

As can be seen from Table 2, compiled according to the load-signal dependence established on the basis of the factory specs of the SC2-5 sensor (Fig. 3), the values of the **U_{Ref}** voltage during the loading-unloading stages change linearly as the acting load increases.

Based on the experimental values obtained at the appropriate measurement points presented in Table 2, the functional load-signal dependence determined between the change in the applied load (ton) and the output voltage of the IDT corresponding to the current load and the voltage difference corresponding to the "0" load state **(U_{force} = $U_{average}$ - "0")** is graphically presented in **Fig. 1**.

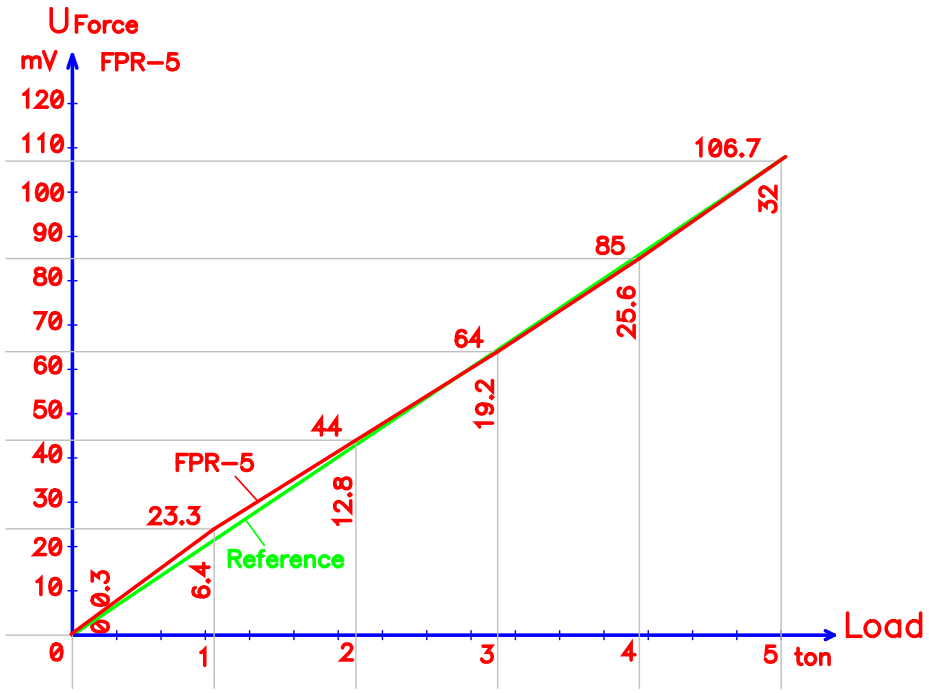

Fig. 10. Load-signal graph of FPR-5 IDT

The calibration of the stroke (acceleration) channel of the FPR-5 IDT was carried out based on the data determined as a result of the experiment in **Table 3.** At the same time, the experimentally obtained voltage signal **(V)** and the corresponding gravitational acceleration (**g**) values were taken into account. The presented data allow determining the functional dependence between the analog signal voltage at the output of the transducer and the real physical quantity - acceleration (**Fig. 11)**.

Table 3

K-8315A acceleration sensor up and down measurements

Measure Point Number, i	Gravity ACC, g	K-8315A stroke measurements at the Ain3 input of the controller were carried out under the following conditions: Supply voltage 12VDC; Output voltage +1.65V+/−1.65V, max acceleration limit +/−10g.						**$U_{average}$**
		U_U1, mV	U_U2, mV	U_U3, mV	U_D1, mV	U_D2, mV	U_D3, mV	$U_{average}$, mV
1	-6	0.33	0.33	0.33	0.33	0.33	0.33	0.33
2	-4	0.77	0.77	0.77	0.77	0.77	0.77	0.77
3	-2	1.21	1.21	1.21	1.21	1.21	1.21	1.21
4	0	1.65	1.65	1.65	1.65	1.65	1.65	1.65
5	+2	2.09	2.09	2.09	2.09	2.09	2.09	2.09
6	+4	2.53	2.53	2.53	2.53	2.53	2.53	2.53
7	+6	2.97	2.97	2.97	2.97	2.97	2.97	2.97

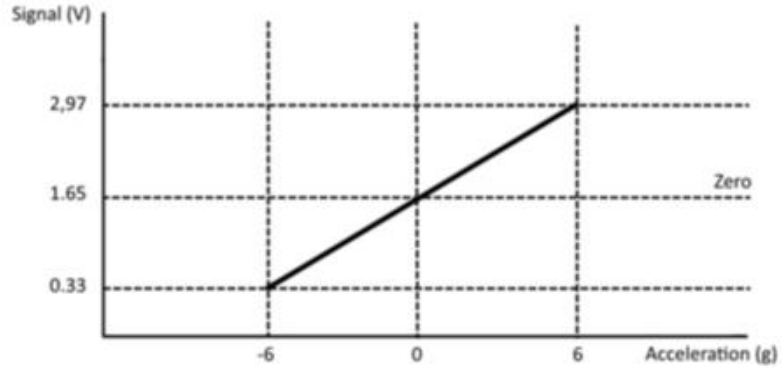

Fig. 11. Stroke-signal graph of FPR-5 IDT

5. Conclusion

The FPR-5 type inter-crosshead IDT, developed as a result of research on sensor, microcontroller and radio frequency technologies, functionally surpasses previous models and has a number of technical advantages in terms of both structural and operational characteristics:

1. The device is designed for inter-traverse mode, the force and stroke sensors are placed in the same housing, as a result of which electromagnetic effects are eliminated and measurement accuracy is increased;

2. The proposed controller module based on the STM32F103 MC provides high-quality processing and transmission of dynamometer chart data with high measurement accuracy, calculation speed, and large memory capacity based on developed processing algorithms;

3. Low energy consumption allows the device to operate on battery power for long periods of time, eliminating the need for an additional power source;

4. Due to the internal temperature and battery voltage monitoring functions, measurement results are regularly adjusted based on their changes to ensure high accuracy.

5. The simplicity of the electrical circuit and the single housing solution reduce the maintenance time of the device and increase operational reliability;

6. Since the FPR-5 IDT is compatible with previous models in terms of mechanical dimensions and installation methods, it can replace existing older dynamometer devices without technical modifications.

Reference

[1] A.X. Mirzəcanzadə, M.Ə. İskəndərov, M.Ə. Abdullayev, R.Q. Ağayev, S.M. Əliyev, Ə.C. Əmirov, Ə.F. Qasımov, Neft və qaz yataqlarının istismarı və işlənilməsi, Bakı, (1960) 444 p. [In Azerbaijani: A.H. Mirzajanzadeh, M.A. Iskenderov, M.A. Abdullayev, R.G. Aghayev, S.M. Aliyev, A.J. Amirov, A.F. Gasimov, Operation and development of oil and gas fields, Baku].

[2] V.T. Məmmədov, O.H. Mirzəyev, Neft mədən texnikasinin təmiri və bərpasi, Bakı, (2012) 285 p. [In Azerbaijani: V.T. Mammadov, O.H. Mirzayev, Repair and restoration of oilfield equipment, Baku].

[3] Ə.H. Əzizov, M.A. Qarayev, H.Ə. Heydərov, S.Ə. Ağammədova, Həcmi hidravlik maşinlar, Bakı, (2010) 601 p. [In Azerbaijani: A.H. Azizov, M.A. Garayev, H.A. Heydarov, S.A. Agammadova, Volumetric hydraulic machines, Baku].

[4] В.В. Андреев, К.Р. Уразаков, В.У. Далимов и др., Справочник по добыче нефти, под ред. К.Р. Уразакова, Москва, ООО “Недра-Бизнесцентр”, (2000) 374 p. [In Russian: V.V. Andreev, K.R. Urazakov, V.U. Dalimov et al., Oil Production Handbook, edited by K.R. Urazakov, Moscow, Nedra-Biznestsentr LLC].

[5] Ас.Г. Рзаев, Интеллектуальный межтраверсный датчик усилия. 32 No.3 (2012) p.158-164. [In Russian: As.H. Rzayev, Intelligent Inter-Crosshead Force Sensor].

[6] STM32F103-BP User Manual

[7] RM0008 Reference manual, STM32F101xx, STM32F102xx, STM32F103xx, STM32F105xx and STM32F107xx advanced Arm-based 32-bit MCUs

[8] F8L10C-10, F8L10-10E LoRa Module Technical Specification V2.0.0

[9] F8L10C Series LoRa Module User Manual V1.0.0

[10] https://kk-group.ru/product/sc2-5/

[11] В.М. Шарапов, Датчики: Справочное пособие, Москва, Техносфера, (2012) 624 p. [In Russian: V.M. Sharapov, Sensors: Reference Guide, Moscow, Tekhnosfera].

[12] А.А. Гуськов, Измерительные преобразователи, Физические основы получения информации, Нижний Новгород. (2008). [In Russian: A.A. Guskov, Measuring Transducers, Physical Fundamentals of Information Acquisition, Nizhny Novgorod].

[13] Kistler K-Beam Accelerometers, Capacitive MEMS, Single-Axis Accelerometer, Type 8315A..., 000-859a-04.13. http://www.helmar.com.pl/helmar/plik/pliki-produktow-kistler_8315_nn4910.pdf

[14] Kistler Accelerometers, Providing quick, accurate and reliable motion data

[15] MPU-6000 and MPU-6050 Product Specification Revision 3.4, https://invensense.tdk.com/wp-content/uploads/2015/02/MPU-6000-Datasheet1.pdf

[16] MPU-6000 and MPU-6050 Register Map and Descriptions Revision 4.2,
https://invensense.tdk.com/wp-content/uploads/2015/02/MPU-6000-Register-Map1.pdf

[17] К.Р. Уразаков, В.В. Андреев, В.П. Жулаев, Нефтепромысловое оборудование для кустовых скважин, Москва, Недра. (1999) pp.80-81. [In Russian: K.R. Urazakov, V.V. Andreev, V.P. Zhulayev, Oilfield equipment for cluster wells, Moscow, Nedra].

[18] J. Karki, Signal conditioning wheatstone resistive bridge sensors, Texas Instruments Incorporated,
SLOA034 – September 1999. https://www.ti.com/lit/an/sloa034/sloa034.pdf

[19] Electrical Circuits, Department of Electrical and Electronics Engineering, Malla Reddy College of Engıneerıng &Technology, (Autonomous Institution – UGC, Govt. of India) https://mrcet.com/downloads/digital_notes/HS/5%20Electrical%20Circuits.pdf

[20] Analysis of ADC System Distortion Caused by Source Resistance. Maxim İntegrated Products

[21] As.H. Rzayev, Y.Q. Əliyev, M.H. Rezvan, Sıxıcı dərəcələmə stendinin yaradılması, Riyaziyyatın tətbiqi məsələləri və yeni informasiya texnologiyaları, 3-cü Respublika elmi konfransı, SDU, Sumqayıt, Dekabr 2016, pp.231-232. [In Azerbaijani: As.H. Rzayev, YG Aliyev, MH Rezvan, Creation of a compression calibration bench, Applied Problems of m$athematics and New Information Technologies, 3rd Republican scientific conference, SDU, Sumgayit, December 2016].

[22] И.Я. Березин, Е.Е. Рихтер, Экспериментальные методы исследований, Раздел "Электромеханические измерения", Челябинск, Издательство ЮУрГУ. (2005) [In Russian: I.Ya. Berezin, E.E. Richter, Experimental Research Methods, Section “Electromechanical Measurements,” Chelyabinsk, South Ural State University Press].

[23] В.М. Коротков, Метрология, стандартизация и сертификация, Москва, Академия, (2004) 368 p. [In Russian: V.M. Korotkov, Metrology, Standardization, and Certification, Moscow, Akademiya].

[24] В.П. Дьяконов, Цифровая обработка сигналов в измерительных системах, СПб., БХВ-Петербург, (2007) 512 p. [In Russian: V.P. Dyakonov, Digital Signal Processing in Measurement Systems, St. Petersburg, BHV-Petersburg].

[25] ASTM E74-18, Standard Practice for Calibration and Verification for Force-Measuring Instruments, ASTM International. (2018)